

# Probabilistic Gabor and Markov Random Fields Segmentation of Brain Tumours in MRI Volumes

N. K. Subbanna and T. Arbel

Centre for Intelligent Machines, McGill University, Montreal, Quebec, Canada

**Abstract.** In this paper, we present a fully automated technique two stage technique for segmenting brain tumours from multispectral human brain magnetic resonance images (MRIs). From the training volumes, we model the brain tumour, oedema and the other healthy brain tissues using their combined space characteristics. Our segmentation technique works on a combination of Bayesian classification of the Gabor decomposition of the brain MRI volumes to produce an initial classification of brain tumours, along with the other classes. We follow our initial classification with a Markov Random Field (MRF) classification of the Bayesian output to resolve local inhomogeneities, and impose a smoothing constraint. Our results show a Dice similarity coefficient of 0.668 for the brain tumours and 0.56 for the oedema.

## 1 Introduction

Brain tumours are a serious health problem, and it is estimated that roughly 100,000 people are diagnosed with brain tumours every years. One of the primary diagnostic and treatment evaluation tools for brain tumours is the magnetic resonance image (MRI) of the brain. A reliable method for segmenting brain tumours would be very useful. However, brain tumours, owing to their extreme diversity of shape, size, type of tumour, etc., present a serious challenge to segmentation techniques. Given the importance of the problem, over the years, there have been a large number of techniques attempted to segment brain tumours automatically. Some of the more important techniques include multilevel segmentation by Bayesian weighted aggregation [1], knowledge based fuzzy techniques [2], and atlas based classification [3]. Wavelet based decompositions are attractive since they are good at capturing large textures of the kind found in brain tumours effectively, and it is unsurprising that there are a few attempts to employ wavelets. One of the more prominent is the wavelet decomposition used in conjunction with support vector machines [4]. In this paper, however, we build on this technique by constructing models not for just the tumours and the oedema, but also for the healthy tissues. We, then, utilise the natural ability of the combined space features to capture the existing patterns to train the machine to recognise the patterns of the tumours, and distinguish it from the other healthy tissues, and provide us with an initial classification. From this initial classification, we then use Markov Random Fields (MRFs) to capture the local label homogeneities and also eliminate false positives that occur due to spurious tumour textures that may arise in other parts of the brain.

## 2 Gabor Bayesian Classification

### 2.1 Training

Our goal is to correctly identify the oedema and the active tumour. During the initial training phase, we first register a tissue atlas to the training volumes obtain the healthy tissues, Grey Matter (GM), White Matter (WM), and Cerebro-Spinal fluid (CSF). We superimpose the tumour and oedema maps provided by the experts to obtain all the classes in the training volumes.

We decompose the training volumes into their constituent Gabor filter bank outputs. The input volumes are the MRI intensity volumes in the four modalities, viz, T1, T2, T1c and FLAIR, so at each voxel, we have a four dimensional vector  $\mathbf{I}_i = (I_i^{T1}, I_i^{T1c}, I_i^{FLAIR}, I_i^{T2})$ . Each image is decomposed to its filter bank output using multiwindow Gabor transforms of the form suggested by [5]. The filter bank outputs are obtained by convolving each modality volume with the Gabor filter bank, which is obtained using the equation

$$h(x, y) = \frac{1}{2\pi\sigma_x\sigma_y} \exp\left(-\frac{1}{2}\left[\frac{x^2}{\sigma_x^2} + \frac{y^2}{\sigma_y^2}\right]\right) \cos(2\pi u_0 x) \quad (1)$$

where  $\sigma_x$  and  $\sigma_y$  are the spreads in the  $x$  and  $y$  directions and  $u_0$  is the modulating frequency. In our case, we choose 4 orientations between 0 and  $\pi$  radians and 5 frequencies. Each chosen frequency is an octave of the previous to ensure that the entire spectrum is covered. We model each class as a Gaussian mixture model, and an 8 component Gaussian mixture suffices to model the different classes in the combined space. We model the Gabor coefficients of all classes, including the tumour and the oedema, using Gaussian mixture models.

### 2.2 Classification

Once the test volume is obtained, it is decomposed into its Gabor filter bank outputs using eqn. (1). The class of each voxel is obtained using Bayesian classification, which is given by

$$P(C_i | \mathbf{I}_i^G) \propto P(\mathbf{I}_i^g | C_i)P(C_i), \quad (2)$$

where  $C$  is a random variable that can take the value of the 5 classes, and  $\mathbf{I}_i^G = I_i^0, I_i^1, \dots, I_i^{R-1}$  is the set of  $R$  Gabor coefficients of the particular voxel  $i$ . It is our experience that the active tumours are quite correctly determined by the Gabor Bayesian technique, but there are often false positive oedema segmentations in regions that mimic the presence of oedema.

## 3 Markov Random Field Classification

The first Bayesian classification results in tumour candidates. We refine this classification by building an MRF based model. We focus on both the intensities

of the voxels and the intensity differences as contrasts are much more consistent. The MRF model is based on the intensity of the voxel, the spatial intensity differences and the class of neighbouring voxels. This can be written as

$$P(C_i | \mathbf{I}_i, \mathbf{I}_{N_i}) = P(\mathbf{I}_i | C_i)P(C_i) \sum_{C_{N_i}=0}^{M-1} P(\Delta\mathbf{I}_{N_i} | C_i, C_{N_i})P(C_{N_i} | C_i) \quad (3)$$

where  $C_{N_i}$  are the classes of the neighbours of  $i$ ,  $\Delta\mathbf{I}_{N-I} = \mathbf{I}_{N_i} - \mathbf{I}_i$ .

### 3.1 Training

Here, we build the intensity distributions of the classes and model them using multivariate Gaussian models. For the neighbourhood, we consider an 8 neighbourhood around the voxel in axial plane and the corresponding voxels in the slices above and below, and build the distributions of each pair, triplet and quadriplet of classes that have an edge or vertex in common in the defined neighbourhood using multivariate Gaussian models. This allows us to model all neighbourhood relations completely in both a mathematical and a practical sense. We use the initial Gabor classification as the prior with the oedema probabilities falling sharply away from the tumour for the second phase.

### 3.2 MRF Classification

We need to compute  $P(\mathbf{C} | \mathbf{I})$  where  $\mathbf{C}$  is a configuration of the labels of all the voxels in the volume and  $\mathbf{I}$  is the set of intensities across all the modalities for all the voxels in the configuration. A sound method of computing  $P(\mathbf{C} | \mathbf{I})$  is by considering the problem as an MRF, which suggests that all class labels are dependent only on their local neighbourhood. Using eqn. (3), we can obtain the energy function for the configuration of labels in the volume with

$$U(\mathbf{C}) = \sum_{i=0}^{Z-1} (\mathbf{I}_i - \mu_{C_i})^T \Sigma_{C_i}^{-1} (\mathbf{I}_i - \mu_{C_i}) + \sum_{N_i} (\Delta\mathbf{I}_{N_i} - \mu_{C_{N_i}, C_i})^T \Sigma_{C_{N_i}, C_i}^{-1} (\Delta\mathbf{I}_{N_i} - \mu_{C_{N_i}, C_i}) + \alpha m(C_{N_i}, C_i), \quad (4)$$

where  $\Delta\mathbf{I}_{N_i} = \mathbf{I}_{N_i} - \mathbf{I}_i$ ,  $m(C_{N_i}, C_i) = 1$  if  $C_{N_i} = C_i$ ,  $Z$  is the total number of voxels, and 0 otherwise, and  $\alpha$  is the weighting coefficient vector. To maximise  $P(\mathbf{C})$ , we use iterated conditional modes (ICM) [6] to minimise  $U(\mathbf{C})$ , where  $\mathbf{C}_{min} = \operatorname{argmin}_{\mathbf{C} \in \mathcal{F}} U(\mathbf{C})$ , and  $\mathcal{F}$  is the set of all possible label configurations.

## 4 Results

In Fig. 1, we compare the results of the two slices where our results are compared against those of the experts' segmentation. In both cases, it can be seen that our results are comparable to the experts' comparison.

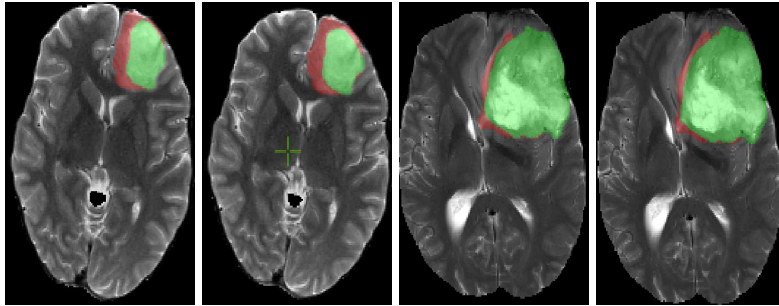


**Fig. 1.** (a) Expert labelling of slice 81 of the volume LG0015 and (b) its corresponding algorithmic labelling. (c) Similarly, the expert labelling of slice 93 of the volume HG0015 and (d) its corresponding labelling by the algorithm. As may be seen, visually, our algorithm’s performance is very close to the experts’ evaluation.

Quantitatively, we train our algorithm on 29 volumes given and test it on the remaining one in a leave one out fashion. We get a Dice similarity coefficient of  $0.561 \pm 0.118$  for the oedema and  $0.668 \pm 0.126$  for the active tumour when we compare our segmentation against those of experts.

## References

1. J. J. Corso, et. al., “Efficient Multilevel Brain Tumour Segmentatin with Integrated Bayesian Model Classification”, *IEEE Trans. Med. Imag.*, Vol. 27(5), pp. 629-640.
2. M. C. Clark et. al., “Automatic Tumour Segmentation using Knowledge Based Techniques”, *IEEE Trans. Med. Imag.*, Vol. 17(2), pp. 187-201.
3. M. Kaus et. al., “Adaptive Template Moderated Brain Tumour Segmentation in MRI”, *Bildverarbeitung fur die Medizin*, pp. 102-106.
4. G. Farias et. al., “Brain Tumour Diagnosis with Wavelets and Support Vector Machines”, in *Proc. 3rd Int. Conf. Intell. Systems and Knowledge Engg.*, 2008.
5. A. K. Jain, and F. Farrokhnia, “Unsupervised Texture Segmentation Using Gabor filters” *Pattern Recognition*, Vol. 24(12), pp. 1167-1186, 1991.
6. R. O. Duda, P. E. Hart, and D. G. Stork, “Pattern Classification”, John Wiley and Sons, 2000.